Impacts of assimilating GOES-16 clear air and cloudy radiance observations on rapidly initiating supercell prediction

Aaron Johnson, Xuguang Wang

Krishna Chandramouli

Multiscale data Assimilation and Predictability (**MAP**) laboratory

School of Meteorology, University of Oklahoma

Jason Otkin (CIMSS, U. Wisconsin)

Thomas Jones (CIMMS, U. Oklahoma)

Jefferey S. Whitaker (NOAA/ESRL/PSD)

27 July 2020

UFS Virtual Workshop

Background and motivation

- High time/space resolution of ABI radiances are particularly appealing for convective scale prediction.
- Direct radar reflectivity assimilation has shown good results for already-initiated storms (e.g., Dowell et al. 2011; Johnson et al. 2015; Wang and Wang 2017).
- Studies have shown that ABI radiances can be directly assimilated to add lead time to NWP of rapidly developing storms (e.g., Cintineo et al. 2016; Zhang et al. 2018, 2019).
- For this study, we have implemented direct ABI all sky radiance assimilation in GSI-EnKF with various methods to enhance the assimilation.
- While ABI has 16 total channels, past studies have focused on single-channel assimilation --> Herein, we start to consider complementary aspects of different channels.
- This presentation will focus on the impact of additive noise inflation and adaptive observation error, impacts of assimilating ABI channel 9 (6.93 micron) vs. channel 10 (7.34 micron), and a brief discussion of ongoing efforts of comparing different bias correction methods.

18 July 2017 Case Study Overview

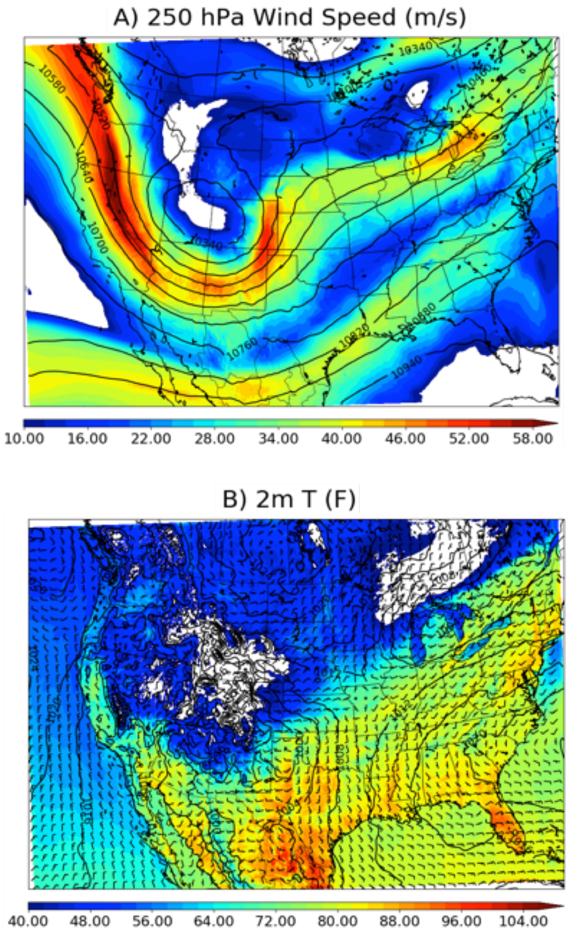

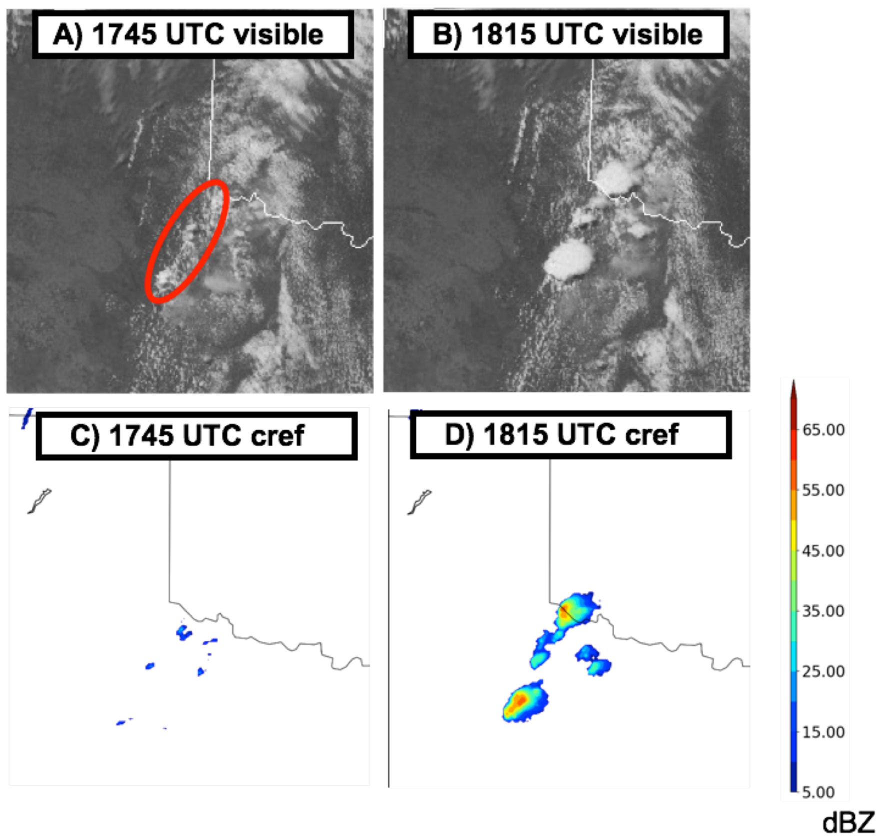

- Western U.S. trough supportive of convection in warm/moist air mass east of dryline in southern Plains.
- Storms initiate by 1815 UTC in terms of high reflectivity cores.
- Deepening cumulus seen in satellite imagery at least 30 minutes prior.

18 July 2017 Case Study Overview

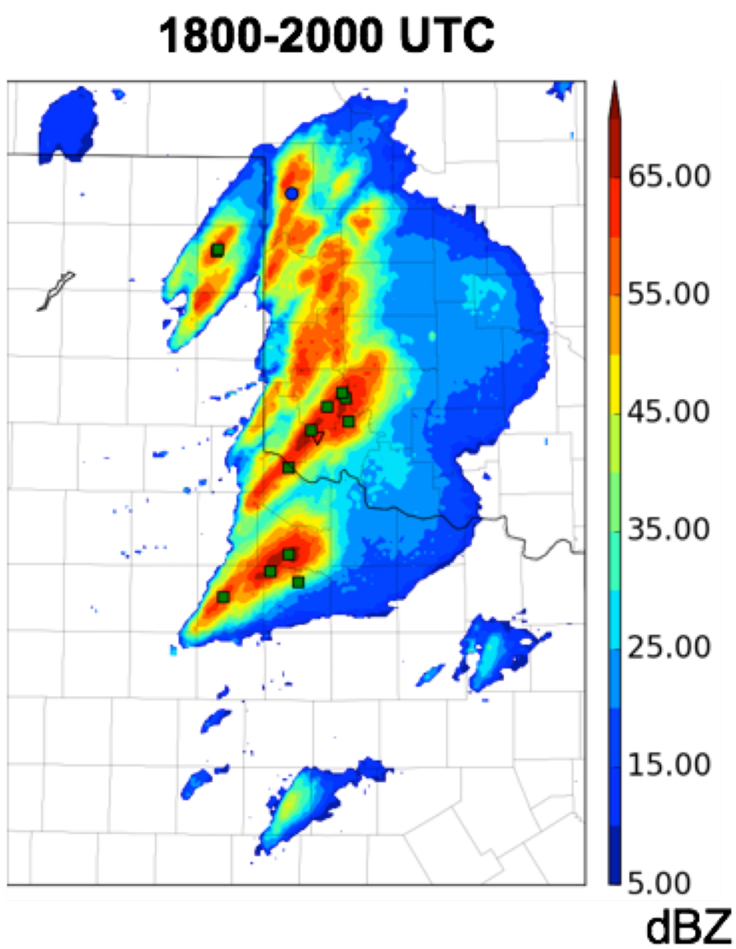

Observed composite reflectivity swath (i.e., maximum during time period)
Severe reports overlaid.

- Primary focus of this study is on forecasts of two long-track supercells.
- Data Assimilation throughout the period prior to and during CI.
- Forecasts initialized at 1800, 1810, 1820 and 1830 UTC.

Experiment Design

- CONUS domain with 3 km grid spacing and LBCs from global ensembles.
- GSI-based EnKF extended for convective scales (Johnson et al. 2015, Wang and Wang 2017)
  - 40-member fixed physics ensemble
  - Hourly assimilation of conventional surface and upper air observation from 0000-1600 UTC on 18 May 2017.
  - 10-minute cycles of radar reflectivity only from 1610-1700 in all experiments to suppress spurious convection in the area.
  - 10-minute cycles of DA of radar reflectivity and ABI mid/low-level water vapor channels from 1710-1830 UTC.
- Vertical localization is ~6km, horizontal is 15 km for both ABI radiance and radar reflectivity.
- Relaxation to Prior Spread covariance inflation applied after DA update.
- O-B QC is turned off to allow large innovations in rapidly developing convection.
- Preprocessing includes parallax correction and removal of partial cloudy observations (5% < cloud fraction < 95%).
- Initially, observation error is 5 dBZ and 1 K for reflectivity and radiance, respectively. Experiments with adaptive observation error for ABI will be shown.
- Radiance bias correction depends on clear sky or cloudy sky

Table of Experiments

Experiment	Add. Noise?	Radar DA?	ABI Ch. 9 DA?	ABI Ch.10 DA?	ABI obs. err.
ch10	N	Y	N	Y	1 K
Ch10_addn	Y	Y	N	Y	1 K
Ch9_addn_oberr	Y	Y	Y	N	adaptive
Ch10_addn_oberr	Y	Y	N	Y	adaptive
Ch9ch10_addn_oberr	Y	Y	Y	Y	adaptive

- Channel 10 is used to show impacts of additive noise and adaptive observation error.
- Experiment using these techniques are used to compare channel 9 and channel 10 impacts.

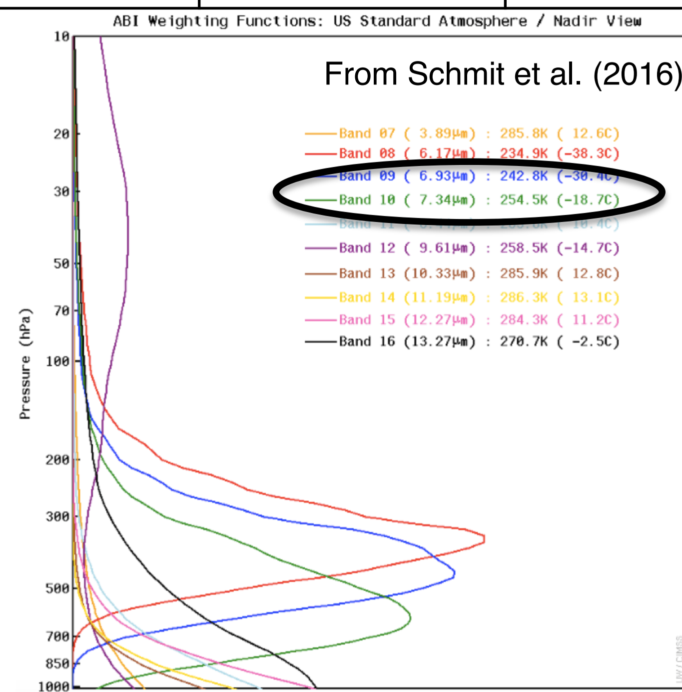

Adaptive observation error

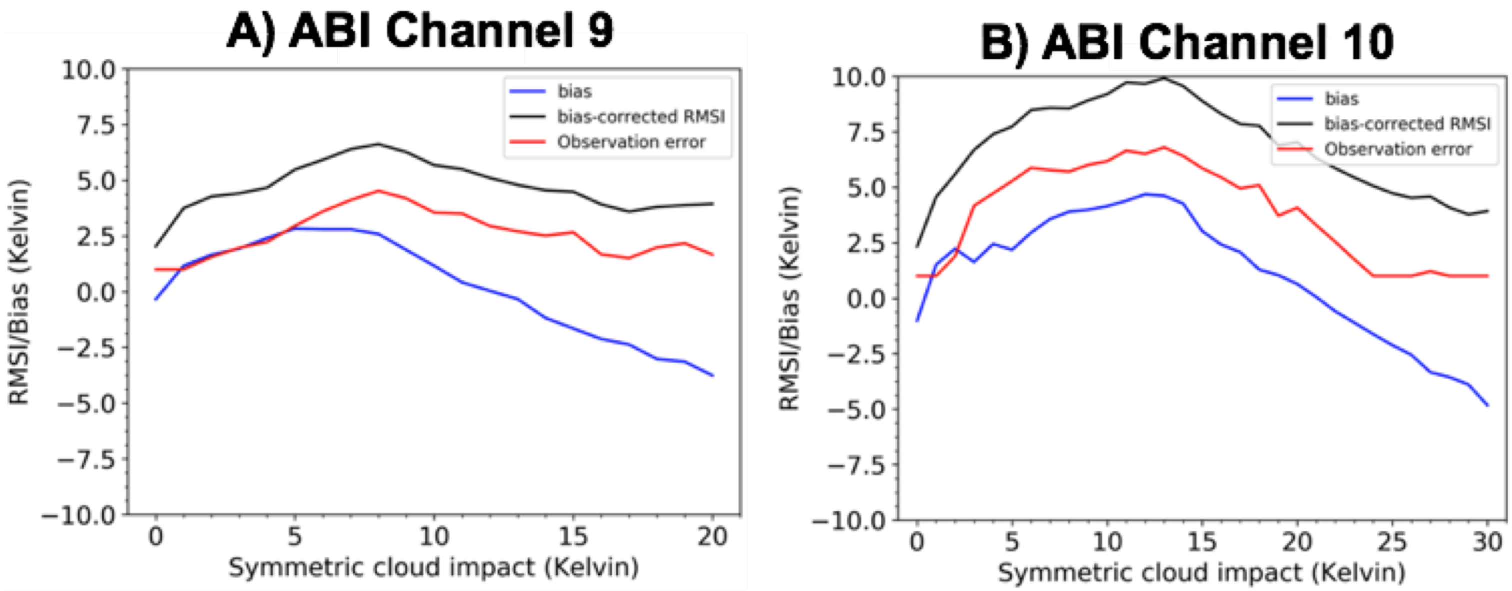

- Differences between simulated Brightness Temperature (BT) and clear-air component of BT in model first guesses are used to determine thresholds of BT for each channel to separate clear/cloudy pixels (Harnisch et al. 2016).
- Difference from this threshold is the “cloud impact” for both first guess and observation radiances.
- Observation error is the residual of bias-corrected RMSI minus bias in each bin of symmetric (i.e., obs/model average) cloud impact.

Radiance DA diagnostics

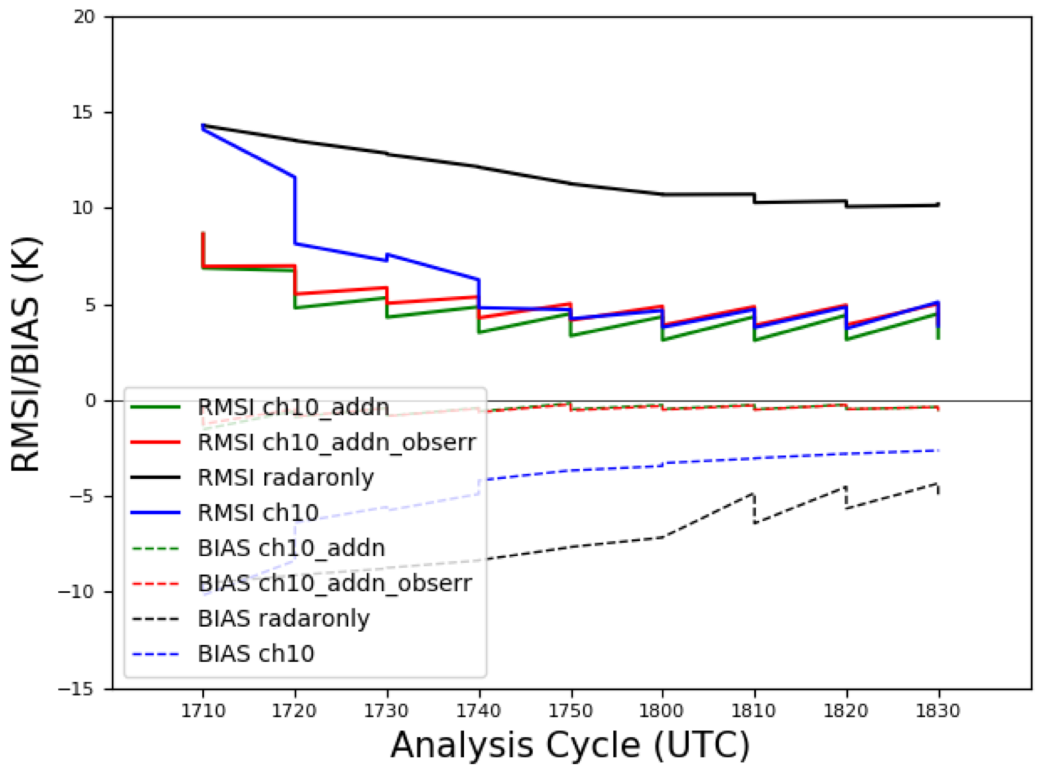

- DA of ch10 (blue lines) reduces RMSI/bias in radiance ch10 space compared to radaronly (black lines)
- Additive noise (green line) gives even better fit to observations.
- Fit to radiance observations not quite as good as green line when adaptive observation error is added (red line)

Verification of deterministic forecasts of 35 dbZ reflectivity

A) 1810 UTC init.

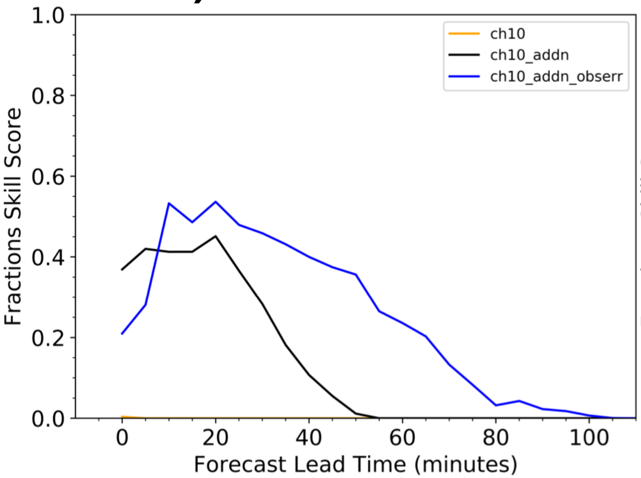

B) 1820 UTC init.

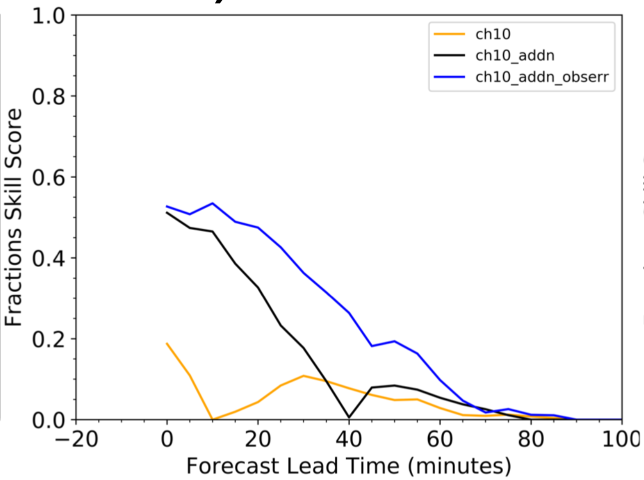

C) 1830 UTC init.

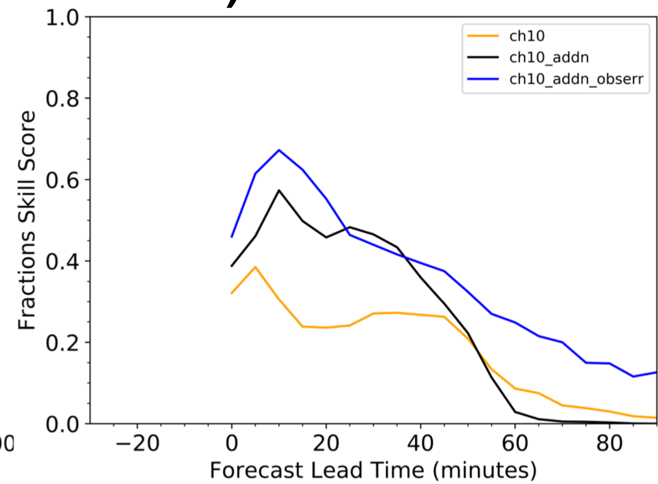

Only ch10_addn and ch10_addn_obserr have any skill.

ch10_addn_obserr has more skill than ch10_addn.

ch10 starts to show a little skill, but overall similar trends as 1800 UTC initialization.

ch10_addn has more skill than ch10 during first ~45 min of forecast.

ch10_addn_oberr maintains a skill advantage throughout the 100 minute forecast.

Verification of deterministic forecasts (reflectivity)

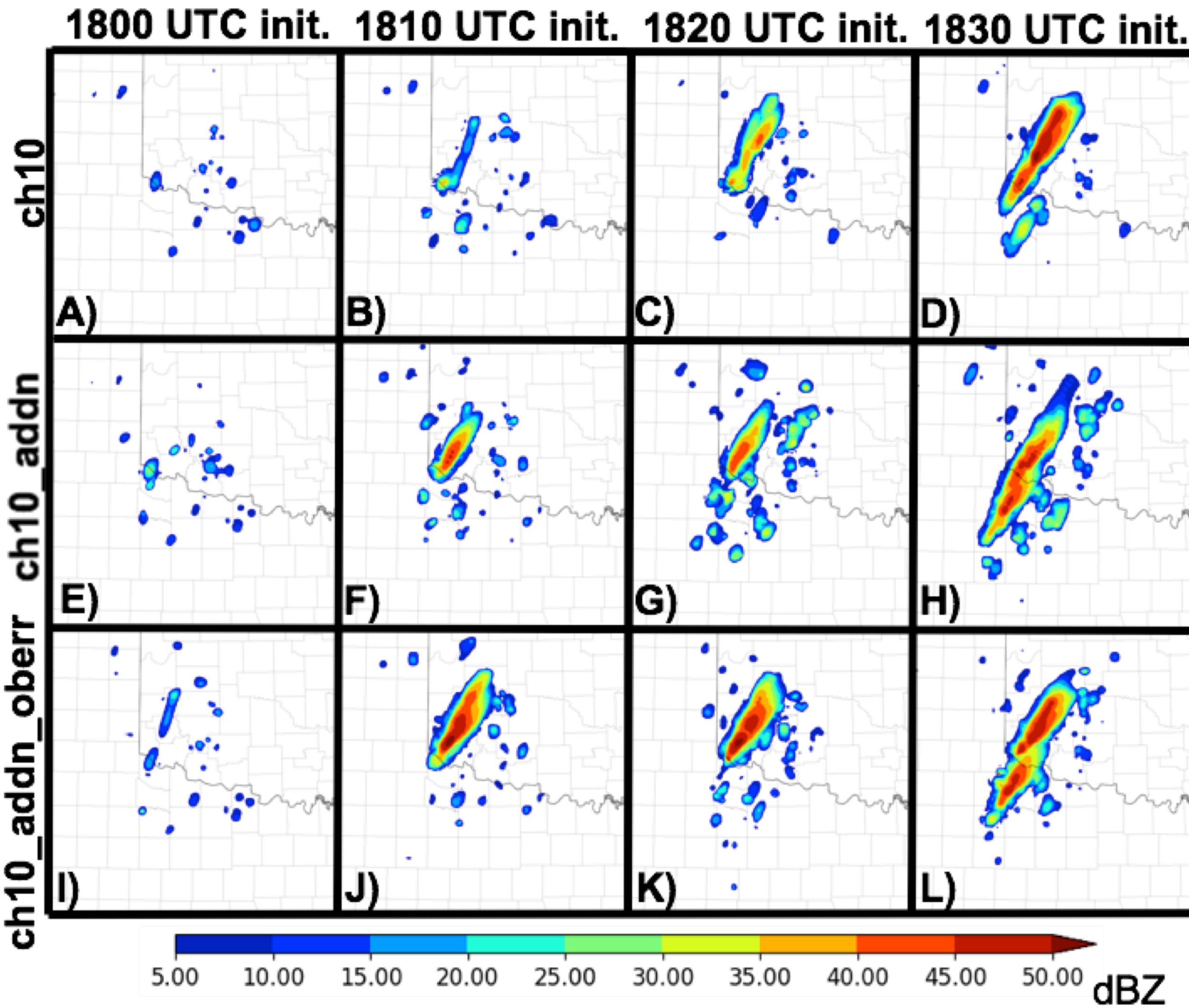

Maximum composite reflectivity between initialization and 2000 UTC

- Additive noise allows DA to pick up on northern storm a few cycles earlier and picks up on separate southern storm.
- Adaptive observation error makes the forecast storms stronger, more consistent with observations.
- All experiments don't pick up southern storm until the 1830 initialized forecast.

Verification of deterministic forecasts (updraft helicity)

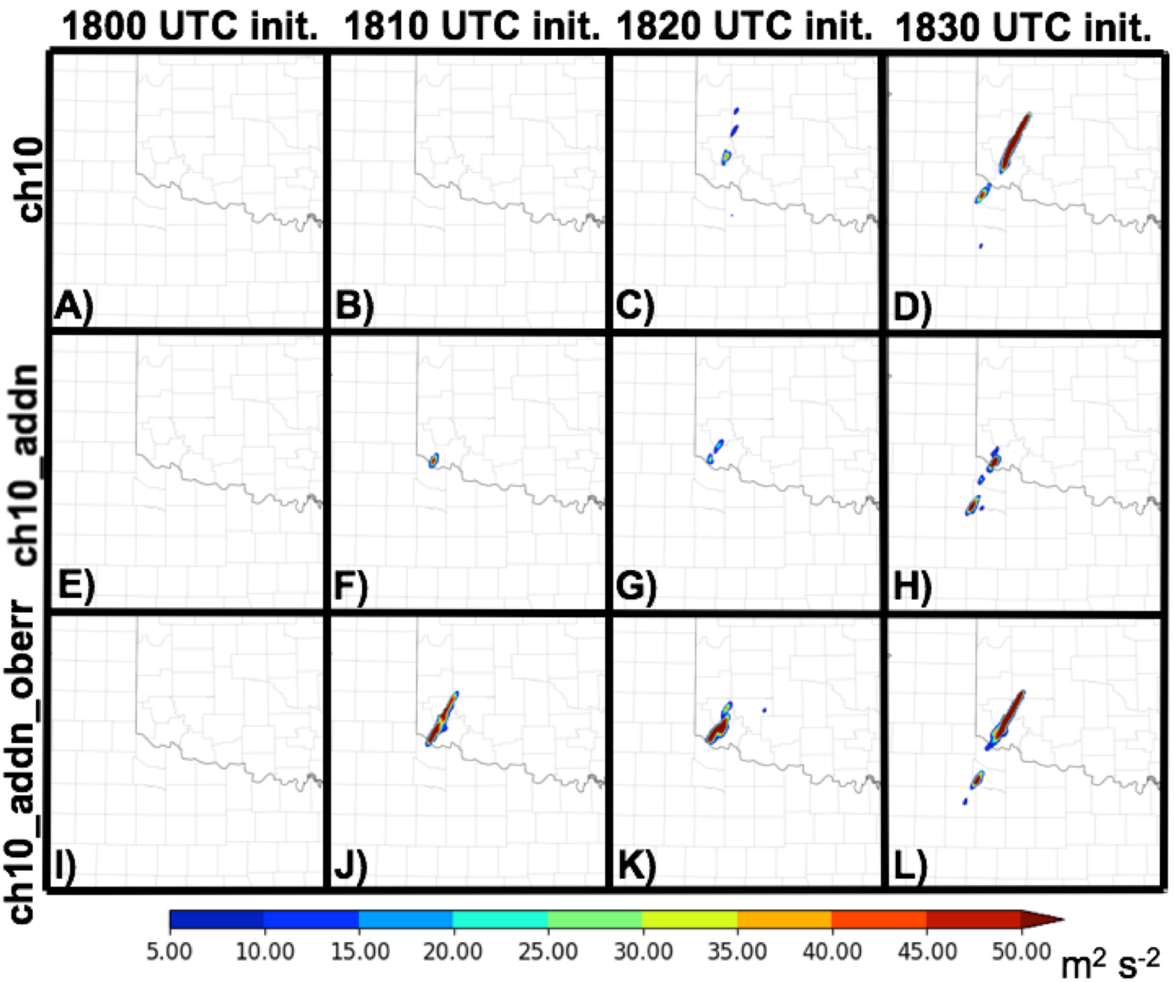

Maximum updraft helicity between initialization and 2000 UTC

- Benefit of adaptive observation error is more clear in updraft helicity swaths.
- Storms are better organized and persist longer, consistent with earlier objective metrics

Additive Noise impact

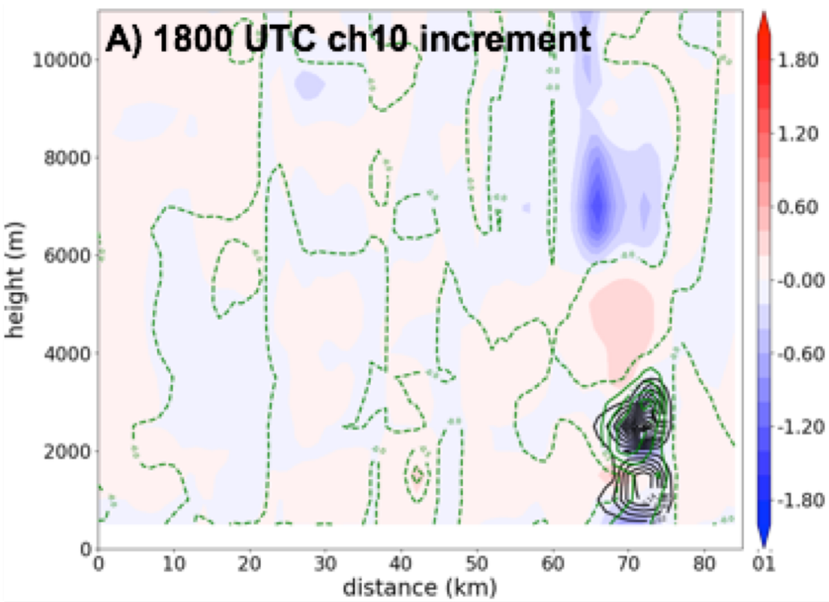

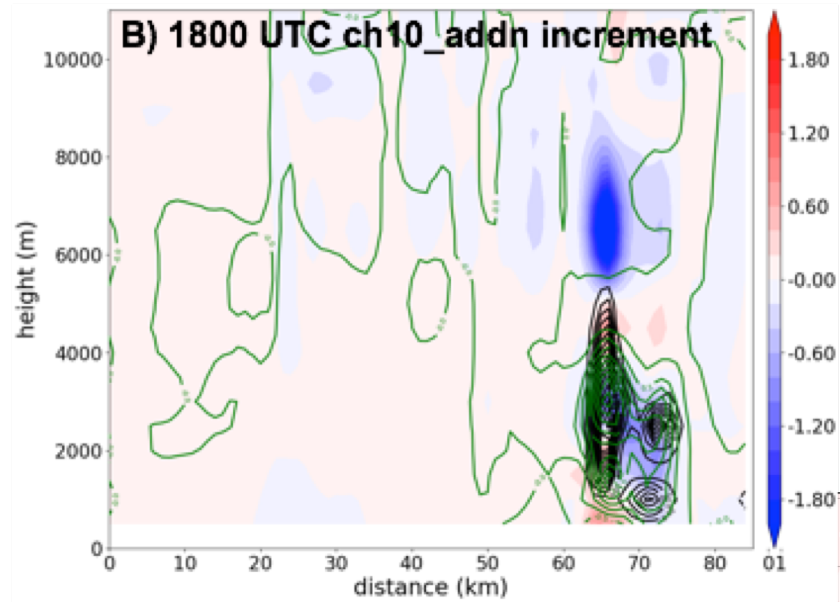

DA increment to Temperature (shading), mixing ratio (green lines), and cloud condensate (black lines)

- The additive noise mitigates insufficient spread/covariance in background ensemble.
- Resulting increment is deeper and more consistent with storm structure when additive noise is used.

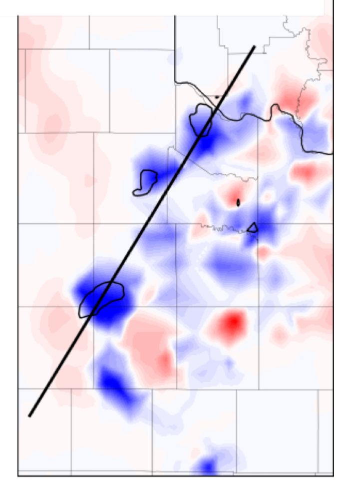

Radiance increment at 1800 UTC In ch10_addn

Adaptive Observation Error impact

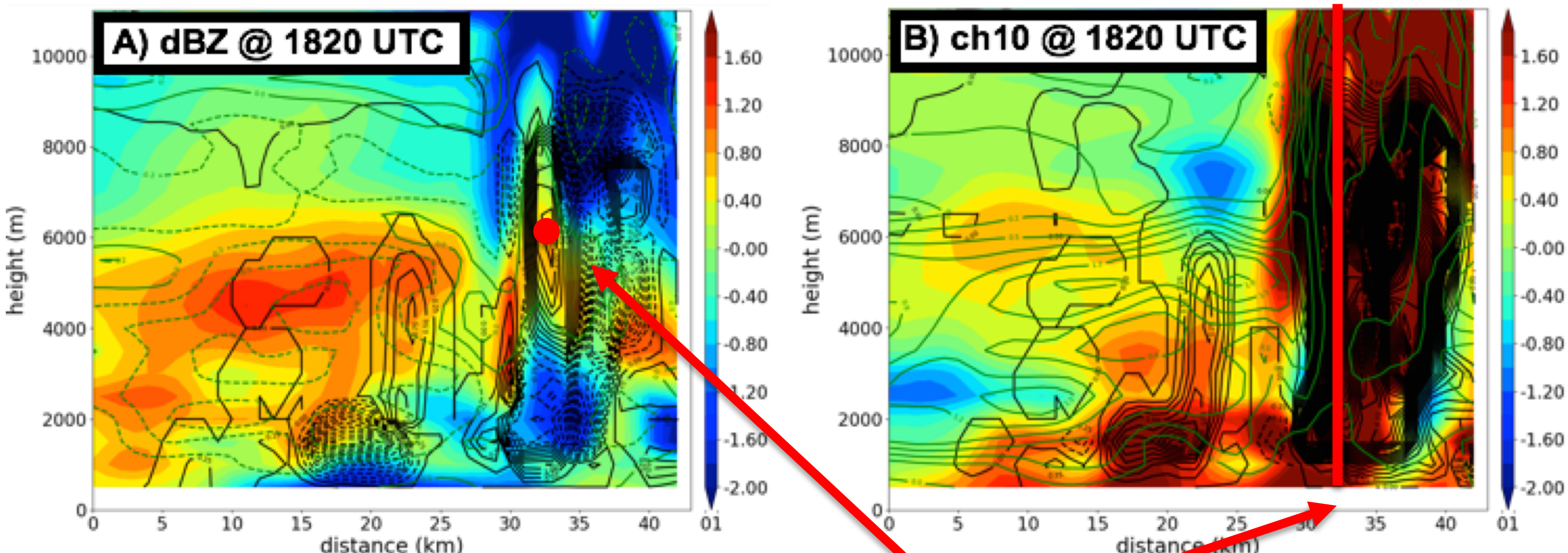

BG ensemble covariance between priors at red dot (right) and temperature (shading), moisture (green lines) and cloud condensate (black lines).

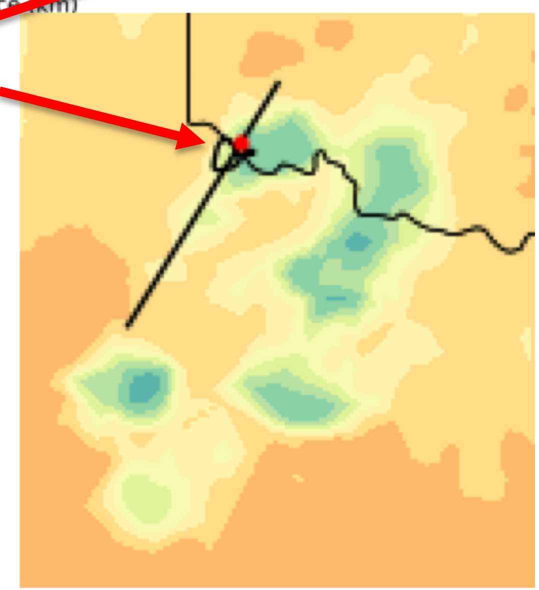

- The ABI radiances are most helpful very early in the CI process.
- After the storm starts to mature (e.g., by 1830 UTC), the ABI only sees the colder anvil than simulated and wants to strengthen the storm over a broad and deep area (right).
- The reflectivity background error covariance is more focused on only strengthening the updraft.
- The adaptive observation error allows the DA to give greater weight to the radar observations as the storm matures and anvil spreads.

Channel 9 vs 10 deterministic forecasts

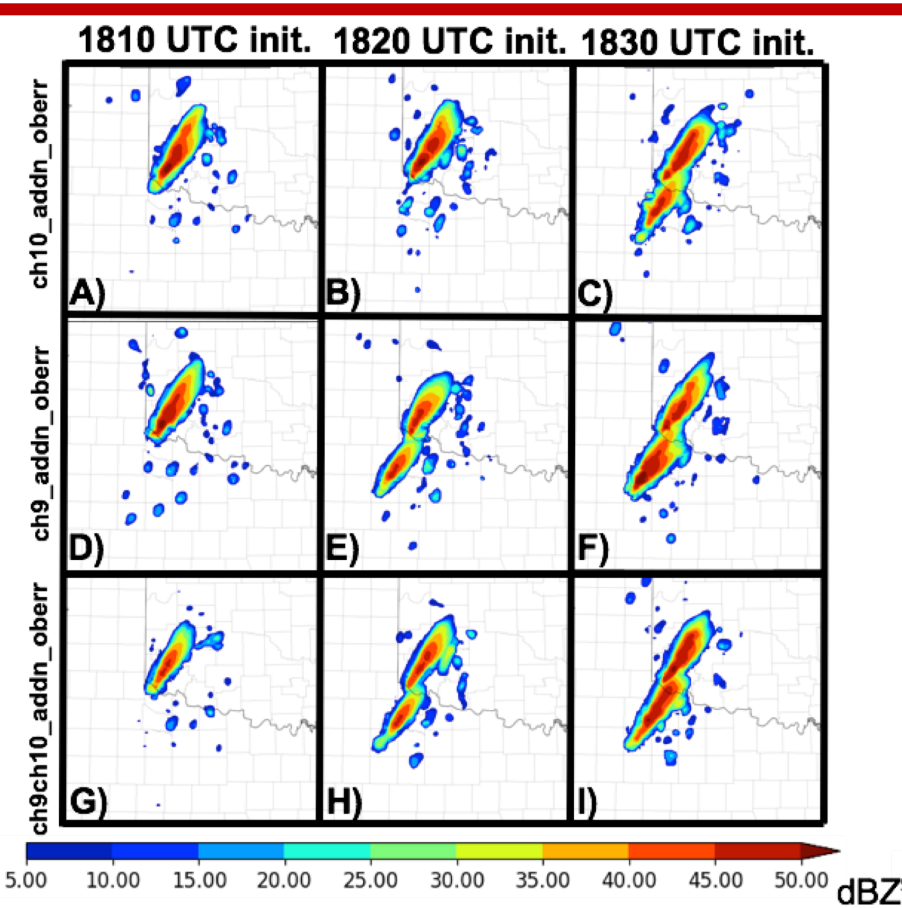

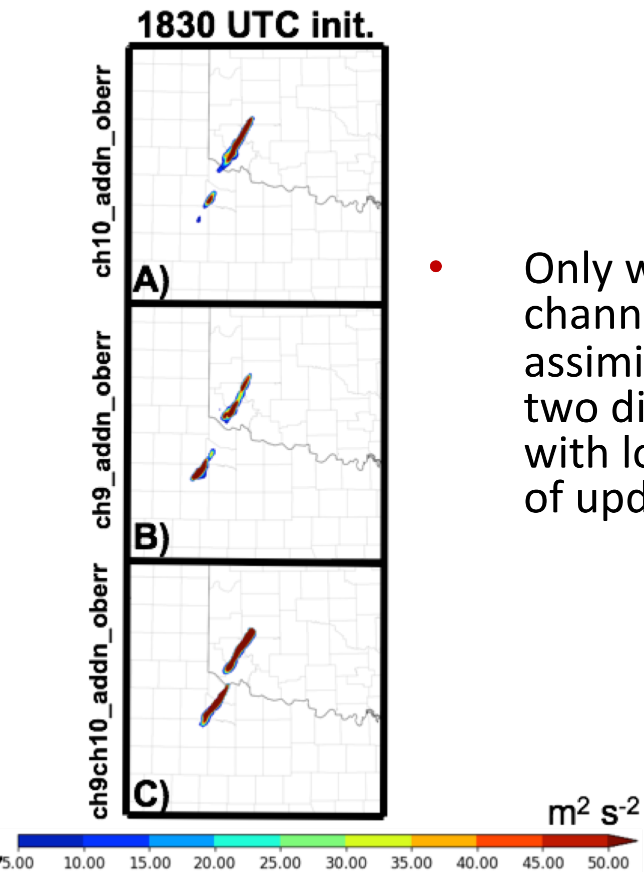

- Only when both channels are assimilated do we get two discrete supercells with long-track swaths of updraft helicity.

- ABI Channel 9 DA initializes the southern storm 10 minutes (1 cycle) earlier than ABI channel 10 DA.
- Assimilating both together has little impact on reflectivity forecast compared to just assimilating channel 9.

Channel 9 vs 10 impact on upper level forcing in clear air

- Channel 9 strengthened the upstream disturbance in clear air through its correlation to water vapor in the layer that channel 9 is sensitive to.
- Therefore, the background ensemble was a little more favorable for members to initiate and maintain the southern storm in the channel 9 experiment.

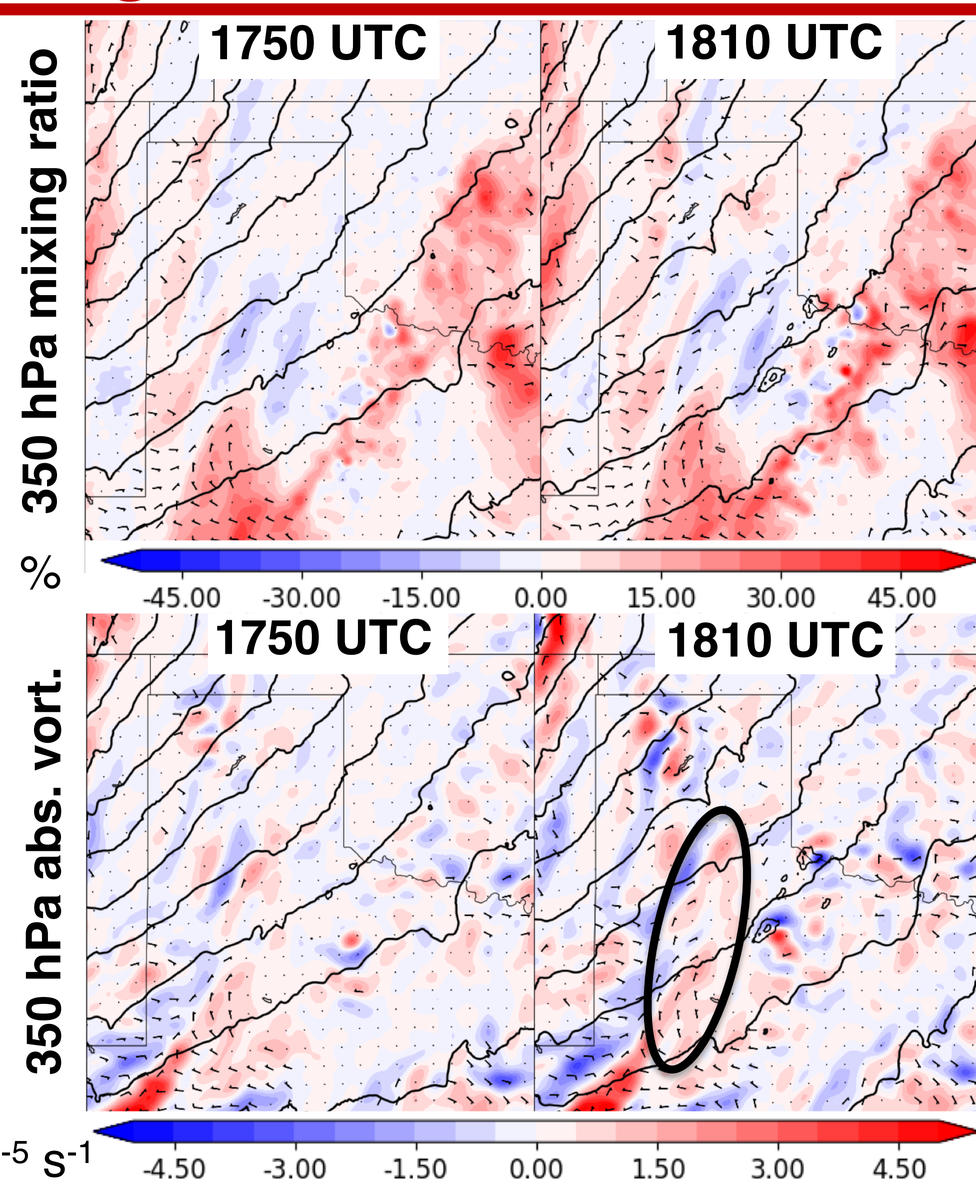

Difference of ch9_addn_obserr background mean from ch10_addn_obserr

$x10^{-5}$ s^{-1}

Evaluation of Different Bias Correction Approaches

- ❑ Theoretical difference based on simple toy model (Eyre 2016) shows that in the presence of model bias and suitable anchor observation, online bias correction will result in a less biased first-guess/analysis state

Reflectivity

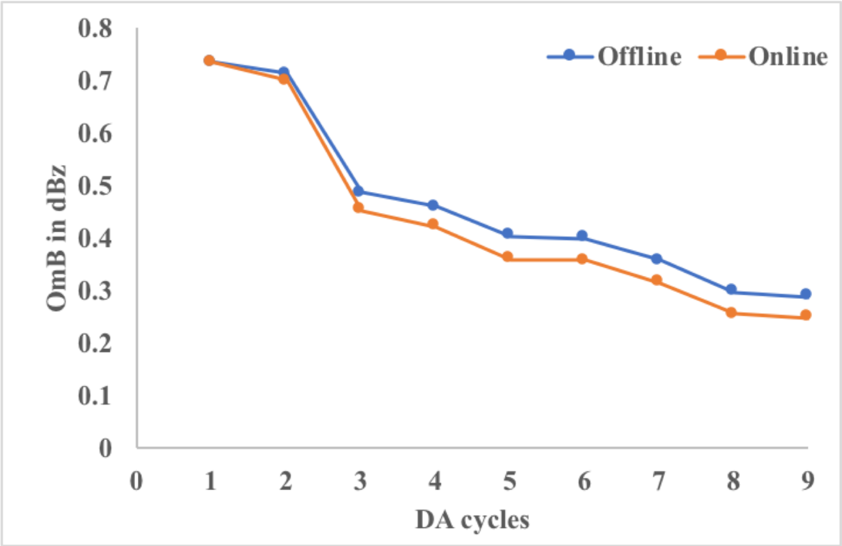

Ch. 10 Radiance

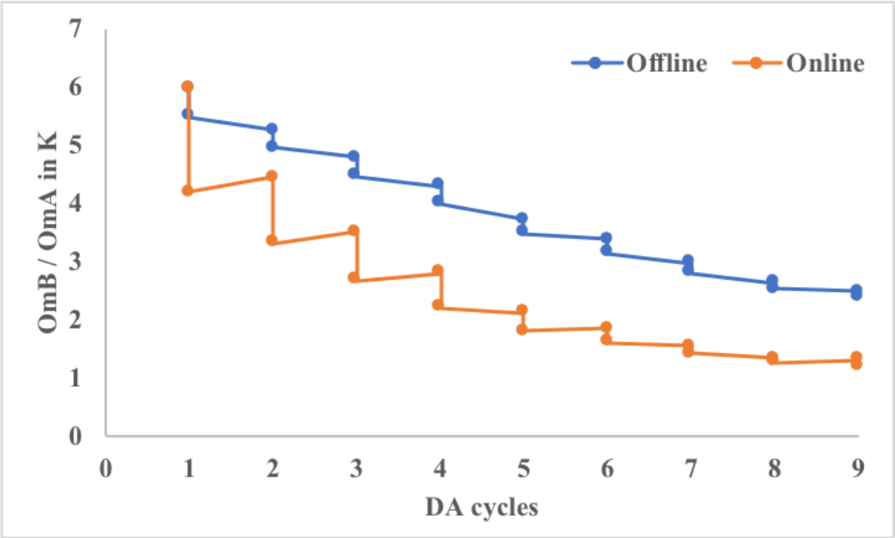

BG/ANL bias using constant bias correction

- From the radar innovation plot and ABI sawtooth plot we observe that the online bias correction experiment results in a less biased background/analysis.

Different Predictors for Non-linear Bias Correction

- Non-linear bias correction is performed using a cubic polynomial function (Otkin et al. 2018) with three different predictors namely (1) Observed BT (2) Simulated BT and (3) Symmetric BT

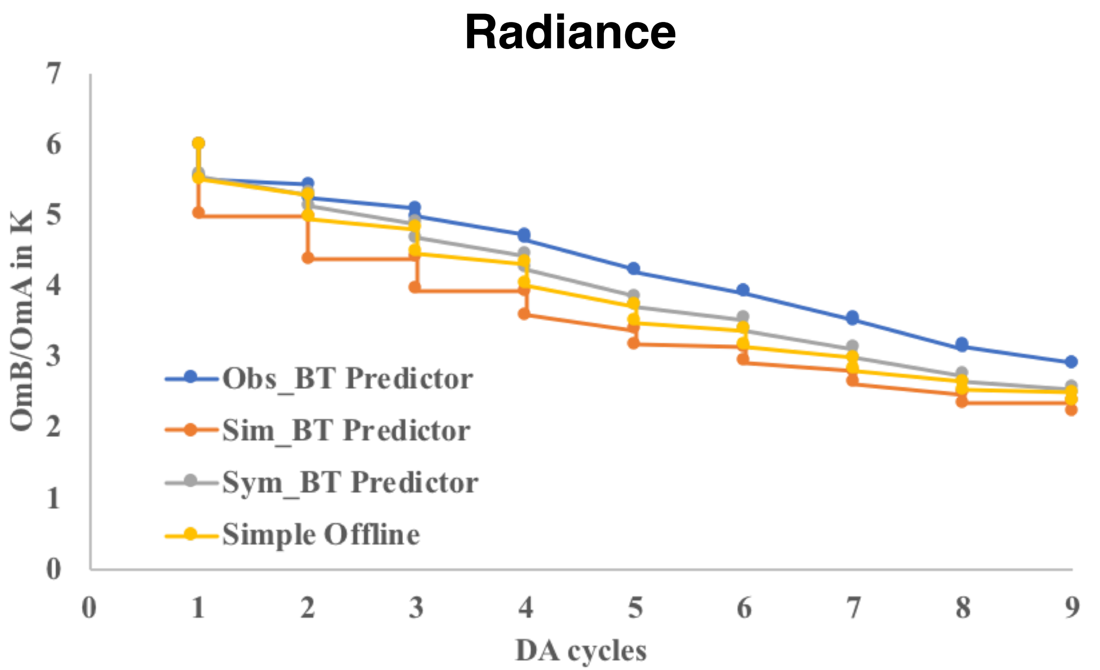

ABI sawtooth plot evaluated over CONUS domain for different bias predictor experiments

Summary and Next Steps

Direct DA of ABI radiances for multiple water vapor channels is implemented in GSI-EnKF.

→ Currently using offline constant bias correction for clear and cloud radiances separately.

→ Additive noise method is adopted from radar DA and implemented for ABI DA.

→ Adaptive observation error based Harnisch et al. (2016) is implemented.

Assimilation of ABI radiances improves short term forecasts during CI of a severe weather event.

→ Additive noise improves forecast lead time of the storms by about 10-20 minutes.

→ Additive noise allows for the assimilation of the southern storm that model first guess previously missed in all ensemble members.

→ Adaptive observation error allows more weight to radar obs that help constrain internal storm structure as it matures and anvil spreads.

→ Channel 9 observations provided further advantages over channel 10 due to observing water vapor at higher level in clear air environment (strengthened shortwave forcing)

→ Best forecast when assimilating both ABI channels.

Ongoing/future work.

→ Impact of implementing a non-linear on-line bias correction technique is being investigated.

→ Additive noise method may need to be further optimized, especially when used together with the additive noise for radar reflectivity DA.

→ Begin UFS implementation with evaluation of radiance channel priors in FV3-SAR